

## SUPPLEMENTARY INFORMATION

### An A<sub>2</sub>-π-A<sub>1</sub>-π-A<sub>2</sub>-type small molecule donor for high-performance organic solar cells

Qian Zhang<sup>a†\*</sup>, Yanna Sun<sup>b†</sup>, Xianjie Chen<sup>a</sup>, Zhijing Lin<sup>a</sup>, Xin Ke<sup>b</sup>, Xiaoyuan Wang<sup>a</sup>, Tian He<sup>a</sup>, Shouchun Yin<sup>a</sup>, Yongsheng Chen<sup>b</sup>, Huayu Qiu<sup>a\*</sup>

<sup>a</sup>College of Material, Chemistry and Chemical Engineering, Hangzhou Normal University, Hangzhou, 311121, P. R. China. \*E-mail: [qzhang@hznu.edu.cn](mailto:qzhang@hznu.edu.cn); [hyqiu@hznu.edu.cn](mailto:hyqiu@hznu.edu.cn).

<sup>b</sup>The Centre of Nanoscale Science and Technology and Key Laboratory of Functional Polymer Materials, State Key Laboratory and Institute of Elemento Organic Chemistry, Collaborative Innovation Center of Chemical Science and Engineering (Tianjin), College of Chemistry, Nankai University, Tianjin, 300071, China.

<sup>†</sup>These authors contributed equally to this paper.

## Table of Contents

1. Characterization .....	3
2. Fabrication and characterization of OSC devices. ....	3
3. Synthesis .....	4
4. Supplementary data.....	8
<b>Fig. S1</b> <sup>1</sup> H NMR spectrum of TBT at 293K in CDCl <sub>3</sub> . ....	8
<b>Fig. S2</b> <sup>13</sup> C NMR spectrum of TBT at 293K in CDCl <sub>3</sub> . ....	8
<b>Fig. S3</b> HRMS spectra of TBT.....	9
<b>Fig. S4</b> <sup>1</sup> H NMR spectrum of DTBTBDD at 293K in CDCl <sub>3</sub> .....	9
<b>Fig. S5</b> <sup>13</sup> C NMR spectrum of DTBTBDD at 293K in CDCl <sub>3</sub> .....	10
<b>Fig. S6</b> HRMS spectra of DTBTBDD. ....	10
<b>Fig. S7</b> <sup>1</sup> H NMR spectrum of DCHOTBTBDD at 293K in CDCl <sub>3</sub> . ....	11
<b>Fig. S8</b> <sup>13</sup> C NMR spectrum of DCHOTBTBDD at 293K in CDCl <sub>3</sub> . ....	11
<b>Fig. S9</b> HRMS spectra of DCHOTBTBDD.....	12
<b>Fig. S10</b> <sup>1</sup> H NMR spectrum of BDD-IN at 293K in CDCl <sub>3</sub> . ....	12
<b>Fig. S11</b> <sup>13</sup> C NMR spectrum of BDD-IN at 293K in CDCl <sub>3</sub> . ....	13
<b>Fig. S12</b> HRMS spectra of BDD-IN. ....	13
<b>Fig. S13</b> (a) TGA curve of BDD-IN. (b) DSC thermograms of BDD-IN with a heating rate of 10 °C min <sup>-1</sup> under N <sub>2</sub> . The lower lines and the upper lines are from the heating scans and cooling scans, respectively. ....	14
<b>Fig. S14</b> Frontier molecular orbitals of BDD-IN using DFT evaluated at the B3LYP/6-31G(d) level of theory. ....	14
<b>Fig. S15</b> Optimized molecular geometries of BDD-IN using DFT evaluated at the B3LYP/6-31G(d) level of theory. ....	14
<b>Fig. S16</b> Chemical structure of PrC <sub>60</sub> MA.....	15

Photovoltaic parameters of BDD-IN:PC <sub>71</sub> BM based devices. ....	15
<b>Fig. S17</b> The statistical histogram of PCEs for BDD-IN:PC <sub>71</sub> BM based devices (20 devices for each case under the as-cast or SVA-treated conditions).....	16
<b>Fig. S18</b> The fitted dark injected current ( $J_{inj}$ ) versus voltage ( $V$ ) for BDD-IN:PC <sub>71</sub> BM devices with different treatment <sup>a</sup> ). ....	16
<b>Fig. S19</b> XRD patterns of pristine BDD-IN films (a) and BDD-IN:PC <sub>71</sub> BM films spin-coated from chloroform onto silicon substrates. Red lines are the fitting lines. ....	17
<b>Fig. S20</b> Experimental dark-current densities for as-cast BDD-IN:PC <sub>71</sub> BM based devices (a) hole mobility (b) electron mobility; SVA-treated BDD-IN:PC <sub>71</sub> BM based devices (c) hole mobility (d) electron mobility. The solid lines represent the fit using a model of single carrier SCLC with field-independent mobility. The $J_D$ - $V$ characteristics are corrected for the built-in voltage $V_{bi}$ that arises from the work function difference between the contacts. ....	18

## 1. Characterization

$^1\text{H}$ -NMR and  $^{13}\text{C}$ -NMR spectra were recorded on a Bruker AVANCE 500 spectrometer. HRMS was performed on Agilent 6530 Accurate-Mass Q-TOF LC/MS Spectrometer using Electro Spray Ionization (ESI) mode. The thermogravimetric analyses (TGA) and differential scanning calorimetric measurements (DSC) were carried out on a TA Q500 and a TA Q2000 instrument under nitrogen gas flow with a  $10\text{ }^\circ\text{C min}^{-1}$  heating rate, respectively. UV-Vis absorption spectra were obtained with JASCO V-570 spectrophotometer. Cyclic voltammetry (CV) measurements were performed with a LK2005A electrochemical workstation in dry THF solution. All CV measurements were carried out at room temperature with a conventional three-electrode configuration employing a glassy carbon electrode as the working electrode, a saturated calomel electrode (SCE) as the reference electrode, and a Pt wire as the counter electrode. THF was distilled from calcium hydride under dry nitrogen immediately prior to use. Tetrabutylammonium phosphorus hexafluoride ( $\text{Bu}_4\text{NPF}_6$ , 0.1 M) in THF was used as the supporting electrolyte, and the scan rate was  $100\text{ mV s}^{-1}$ . AFM was performed using Multimode 8 atomic force microscope in tapping mode.

## 2. Fabrication and characterization of OSC devices.

The photovoltaic devices were fabricated with a structure of ITO/PEDOT:PSS/Donor:PC<sub>71</sub>BM/PrC<sub>60</sub>MA/Al. The ITO coated glass substrates were cleaned by ultrasonic treatment in detergent, deionized water, acetone, and isopropyl alcohol under ultrasonication for 15 min each and subsequently dried by a nitrogen blow. A thin layer of PEDOT:PSS (Clevios P VP AI 4083, filtered at  $0.45\text{ }\mu\text{m}$ ) was spin-coated at 3000 rpm onto ITO surface. After baking at  $150\text{ }^\circ\text{C}$  for 20 minutes, the substrates were transferred into an argon-filled glove box. Subsequently, the active layer was spin-coated from blend chloroform solutions with weight ratio of donor and PC<sub>71</sub>BM at 1:0.8 and then the substrates were placed in a glass petri dish containing  $150\text{ }\mu\text{L}$  chloroform for 70 s for solvent vapor annealing (SVA). Then the substrates were removed. And PrC<sub>60</sub>MA solution (0.5 mg/ml, dissolved in methanol) was spin-coated at 3000 rpm. Finally, 80 nm Al layer were deposited under high vacuum ( $< 2\times 10^{-4}\text{ Pa}$ ). The effective areas of cells were  $4\text{ mm}^2$  defined by shallow masks. The current density-voltage ( $J$ - $V$ ) curves of photovoltaic devices were obtained by a Keithley 2400 source-measure unit. The photocurrent was measured under illumination simulated  $100\text{ mW cm}^{-2}$  AM 1.5G irradiation using a

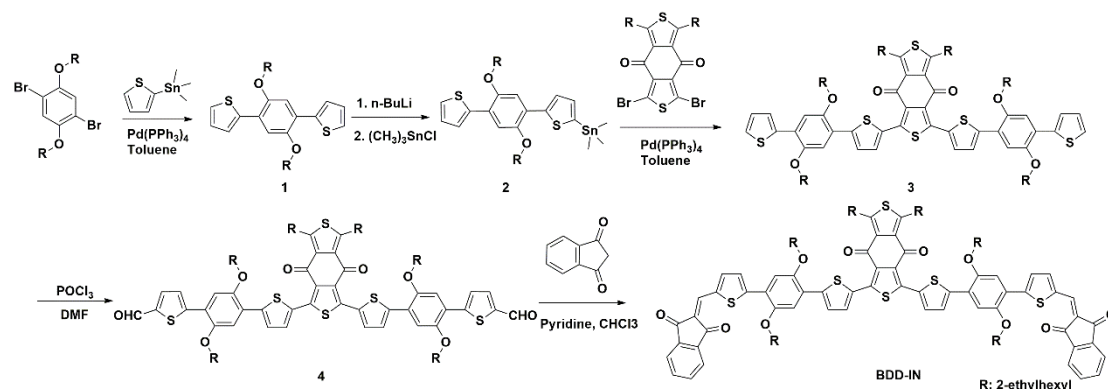
Xenon-lamp-based solar simulator (SAN-EI XES-70S1) calibrated with a standard Si solar cell in an argon-filled glovebox. External quantum efficiencies were measured using a halogen tungsten lamp, monochromator, optical chopper, and lock-in amplifier, and the photon flux was determined using a calibrated silicon photodiode.

Hole-only devices with an architecture of ITO/PEDOT:PSS (40 nm)/BDD-IN:PC<sub>71</sub>BM/Au (100 nm) and electron-only devices with an architecture of glass/Al (100 nm)/ BDD-IN:PC<sub>71</sub>BM /Al (100 nm) were fabricated. The devices were measured using Keithley 2400 source meter in a glove box under dark. The hole and electron mobilities were calculated by fitting the dark current using the modified Mott-Gurney relationship<sup>1, 2</sup>:

$$J = \frac{9\varepsilon_0\varepsilon_r\mu_0V^2}{8L^3} \exp\left(0.89\beta\sqrt{\frac{V}{L}}\right) \quad (1)$$

where  $J$  is the current density,  $L$  is the film thickness of the active layer,  $\mu_0$  is the hole or electron mobility,  $\varepsilon_r$  is the relative dielectric constant of the transport medium,  $\varepsilon_0$  is the permittivity of free space ( $8.85 \times 10^{-12}$  F m<sup>-1</sup>).  $\beta$  is a constant for each device, which could be got by fitting the dark current using the equation.  $V (= V_{\text{appl}} - V_{\text{bi}})$  is the internal voltage in the device, where  $V_{\text{appl}}$  is the applied voltage to the device and  $V_{\text{bi}}$  is the built-in voltage due to the relative work function difference of the two electrodes.

### 3. Synthesis



**Scheme 1** Synthetic routes to target molecule.

2,2'-(2,5-bis((2-ethylhexyl)oxy)-1,4-phenylene)dithiophene (**1**): A solution of 1,4-dibromo-2,5-bis((2-ethylhexyl)oxy)benzene (4.92 g, 10.0mmol) and trimethyl(thiophen-2-yl)stannane (14.93 g, 40.0 mmol) in dry toluene (100 mL) was degassed twice with argon following the addition of Pd(PPh<sub>3</sub>)<sub>4</sub> (4.62 g, 4.0 mmol). After stirring and refluxing for 24 h at 110 °C with the protection of argon, the reaction mixture was poured into water (100 mL) and extracted with dichloromethane (100 mL × 2). The organic layer was washed

with water for twice and dried over anhydrous MgSO<sub>4</sub> for 3 h. The solvent was removed by evaporation under reduced pressure. The crude product was purified by silica gel column chromatography with dichloromethane/petroleum ether (1:2) as eluent to afford **1** as a pale-yellow solid (3.67 g, 7.35 mmol, 74%). <sup>1</sup>H NMR (500 MHz, CDCl<sub>3</sub>) δ 7.61 (dd, *J* = 2.5, 1.2 Hz, 2H), 7.43 – 7.38 (m, 2H), 7.35 (d, *J* = 1.1 Hz, 2H), 7.17 (dd, *J* = 4.0, 1.0 Hz, 2H), 4.06 (d, *J* = 5.4 Hz, 4H), 1.92 (dt, *J* = 6.0 Hz, 2H), 1.64 (tdd, *J* = 7.3 Hz, 6H), 1.47 – 1.34 (m, 10H), 1.06 – 0.97 (m, 12H). <sup>13</sup>C NMR (126 MHz, CDCl<sub>3</sub>) δ 149.38, 139.38, 126.69, 125.60, 125.26, 122.91, 112.71, 39.66, 30.66, 29.16, 24.06, 23.08, 14.13, 11.22. MS (HRMS-TOF) *m/z*: calcd for C<sub>30</sub>H<sub>42</sub>O<sub>2</sub>S<sub>2</sub> 499.2699; found, 499.2695.

(5-(2,5-bis((2-ethylhexyl)oxy)-4-(thiophen-2-yl)phenyl)thiophen-2-yl)trimethylstannane (**2**): *n*-Butyllithium (2.29 mL, 5.5 mmol, 2.4 M) was added dropwise to a solution of TBT (2.49 g, 5.0 mmol) in THF (50 mL) at -78 °C with the protection of argon. After stirring at -78 °C for 3 h, trimethyltin chloride (5.5 mL, 5.5 mmol, 1 M) was added in one portion to the reaction mixture at the same temperature. The solution was stirred at -78 °C for 30 min, slowly warmed to room temperature. After stirring for 24 h, the reaction mixture was poured into water (100 mL) and extracted with dichloromethane (100 mL × 2). The organic layer was washed with water for twice and dried over anhydrous MgSO<sub>4</sub> for 3 h. The solvent was removed by evaporation under reduced pressure. The crude product was obtained in about 90% yield as brown oil and could be used for further reactions without any purification.

1,3-bis(5-(2,5-bis((2-ethylhexyl)oxy)-4-(thiophen-2-yl)phenyl)thiophen-2-yl)-5,7-bis(2-ethylhexyl)-4*H*,8*H*-benzo[1,2-*c*:4,5-*c'*]dithiophene-4,8-dione (**3**): A solution of TBT-Sn (1.32 g, 1.8 mmol, 90%) and BDD-Br (0.36 g, 0.6 mmol) in dry toluene (50 mL) was degassed twice with argon following the addition of Pd(PPh<sub>3</sub>)<sub>4</sub> (0.21 g, 0.18 mmol). After stirring and refluxing for 24 h at 110 °C with the protection of argon, the reaction mixture was poured into water (100 mL) and extracted with dichloromethane (100 mL × 2). The organic layer was washed with water for twice and dried over anhydrous MgSO<sub>4</sub> for 3 h. The solvent was removed by evaporation under reduced pressure. The crude product was purified by silica gel column chromatography with dichloromethane/petroleum ether (1:1) as eluent to afford **3** as a red solid (0.27 g, 0.19 mmol,

31%). <sup>1</sup>H NMR (500 MHz, CDCl<sub>3</sub>) δ 7.90 (d, *J* = 4.0 Hz, 2H), 7.58 (d, *J* = 4.1 Hz, 2H), 7.55 (dd, *J* = 3.6, 0.9 Hz, 2H), 7.36 (dd, *J* = 5.1, 1.0 Hz, 2H), 7.32 (s, 2H), 7.28 (s, 2H), 7.11 (dd, *J* = 5.1, 3.7 Hz, 2H), 4.02 (dd, *J* = 8.9, 5.6 Hz, 9H), 3.36 (dd, *J* = 14.9, 7.1 Hz, 4H), 1.93 – 1.81 (m, 5H), 1.78 (d, *J* = 6.1 Hz, 3H), 1.64 – 1.53 (m, 13H), 1.39 – 1.23 (m, 36H), 0.99 – 0.87 (m, 36H). <sup>13</sup>C NMR (126 MHz, CDCl<sub>3</sub>) δ 177.69, 153.19, 149.73, 149.42, 142.93, 142.65, 139.27, 133.33, 132.64, 130.75, 126.74, 125.93, 125.85, 125.45, 123.59, 122.33, 112.55, 112.36, 71.93, 71.85, 39.69, 39.63, 30.77, 30.68, 29.23, 29.17, 28.86, 26.06, 24.11, 24.07, 23.13, 23.07, 23.03, 14.13, 11.27, 11.24, 10.96. MS (HRMS-TOF) *m/z*: calcd for C<sub>86</sub>H<sub>116</sub>O<sub>6</sub>S<sub>6</sub> 1438.3697; found, 1438.7130.

5,5'-(((5,7-bis(2-ethylhexyl)-4,8-dioxo-4*H*,8*H*-benzo[1,2-*c*:4,5-*c'*]dithiophene-1,3-diyl)bis(thiophene-5,2-diyl))bis(2,5-bis((2-ethylhexyl)oxy)-4,1-phenylene))bis(thiophene-2-carbaldehyde) (**4**): POCl<sub>3</sub> (2 mL) was added dropwise to DMF (5 mL) at 0 °C under the protection of argon. The color of the solution turned into pale orange after stirring for 30 min at 25 °C. Then the mixture was transferred to a solution of **3** (200.0 mg, 0.14 mmol) in 1,2-dichloroethane (30 mL). After stirring and refluxing for 24 h at 70 °C with the protection of argon, the reaction mixture was poured into water (100 mL) and extracted with dichloromethane (100 mL × 2). The organic layer was washed with water for twice and dried over anhydrous MgSO<sub>4</sub> for 3 h. The solvent was removed by evaporation under reduced pressure. The crude product was purified by silica gel column chromatography with dichloromethane/petroleum ether (1:1) as eluent to afford compound **4** as a red oil (187.1 mg, 0.13 mmol, 90%). <sup>1</sup>H NMR (500 MHz, CDCl<sub>3</sub>) δ 9.93 (s, 2H), 7.89 (d, *J* = 4.0 Hz, 2H), 7.76 (d, *J* = 4.0 Hz, 2H), 7.66 (d, *J* = 4.0 Hz, 2H), 7.62 (d, *J* = 4.0 Hz, 2H), 7.35 (s, 2H), 7.31 (s, 2H), 4.04 (dd, *J* = 11.1, 5.6 Hz, 8H), 3.36 (dd, *J* = 14.9, 7.0 Hz, 4H), 1.96 – 1.86 (m, 4H), 1.82 – 1.74 (m, 2H), 1.57 (dt, *J* = 7.2, 6.8 Hz, 12H), 1.38 – 1.22 (m, 36H), 1.00 – 0.87 (m, 36H). <sup>13</sup>C NMR (126 MHz, CDCl<sub>3</sub>) δ 183.08, 177.64, 153.44, 150.16, 149.68, 149.35, 142.52, 142.50, 142.28, 136.13, 134.03, 133.24, 132.84, 130.78, 126.52, 126.24, 124.53, 121.75, 112.46, 112.24, 72.03, 41.35, 39.60, 39.56, 33.67, 32.77, 30.75, 30.73, 29.71, 29.21, 29.15, 28.86, 26.06, 24.11, 24.09, 23.12, 23.06, 23.03, 14.13, 14.10, 11.25, 11.21, 10.96. MS (HRMS-TOF) *m/z*: calcd for C<sub>88</sub>H<sub>116</sub>O<sub>8</sub>S<sub>6</sub> 1494.3383; found, 1494.7028.

2,2'-((((5,7-bis(2-ethylhexyl)-4,8-dioxo-4*H*,8*H*-benzo[1,2-*c*:4,5-*c'*]dithiophene-1,3-diyl)bis(thioph

hene-5,2-diyl))bis(2,5-bis((2-ethylhexyl)oxy)-4,1-phenylene))bis(thiophene-5,2-diyl))bis(methanylylidene))bis(1*H*-indene-1,3(2*H*)-dione) (**BDD-IN**): **4** (149.4 mg, 0.10 mmol) and indenedione (58.5 mg, 0.40 mmol) were dissolved in a dry CHCl<sub>3</sub> (30 mL) solution under the protection of argon, and then three drops of piperidine was added to the mixture. After stirring and refluxing for 12 h, the mixture was extracted with dichloromethane (50 mL × 2), and then the organic layer was washed with water and dried over anhydrous MgSO<sub>4</sub> for 3 h. The solvent was removed by evaporation under reduced pressure. The crude production was precipitated from chloroform/ethanol (*v:v* = 3:10) to afford **BDD-IN** as a black solid (113.8 mg, 0.065 mmol, 66%). <sup>1</sup>H NMR (500 MHz, CDCl<sub>3</sub>) δ 8.26 (d, *J* = 3.1 Hz, 2H), 7.99 – 7.93 (m, 6H), 7.91 (d, *J* = 3.9 Hz, 2H), 7.75 (dt, *J* = 9.6, 6.2 Hz, 6H), 7.64 (t, *J* = 3.8 Hz, 2H), 7.36 (t, *J* = 6.1 Hz, 4H), 4.09 (t, *J* = 5.8 Hz, 8H), 3.37 (dd, *J* = 15.0, 7.1 Hz, 4H), 1.97 (dt, *J* = 11.9, 5.8 Hz, 4H), 1.84 – 1.76 (m, 2H), 1.69 – 1.54 (m, 15H), 1.38 (dd, *J* = 7.1, 5.8 Hz, 35H), 1.03 – 0.86 (m, 36H). <sup>13</sup>C NMR (126 MHz, CDCl<sub>3</sub>) δ 190.65, 186.78, 177.62, 176.19, 153.37, 150.46, 149.74, 142.51, 142.37, 142.16, 140.41, 137.43, 134.85, 134.57, 134.13, 133.25, 132.82, 130.84, 127.56, 126.61, 124.68, 123.96, 122.90, 122.71, 122.14, 112.18, 72.19, 71.99, 41.36, 39.68, 39.56, 33.68, 32.78, 30.83, 30.66, 29.29, 29.17, 28.86, 26.07, 24.16, 24.07, 23.15, 23.08, 23.03, 14.16, 14.14, 11.35, 11.21, 10.97. MS (HRMS-TOF) *m/z*: calcd for C<sub>106</sub>H<sub>124</sub>O<sub>10</sub>S<sub>8</sub> 1750.5176; found, 1750.7548.

#### 4. Supplementary data

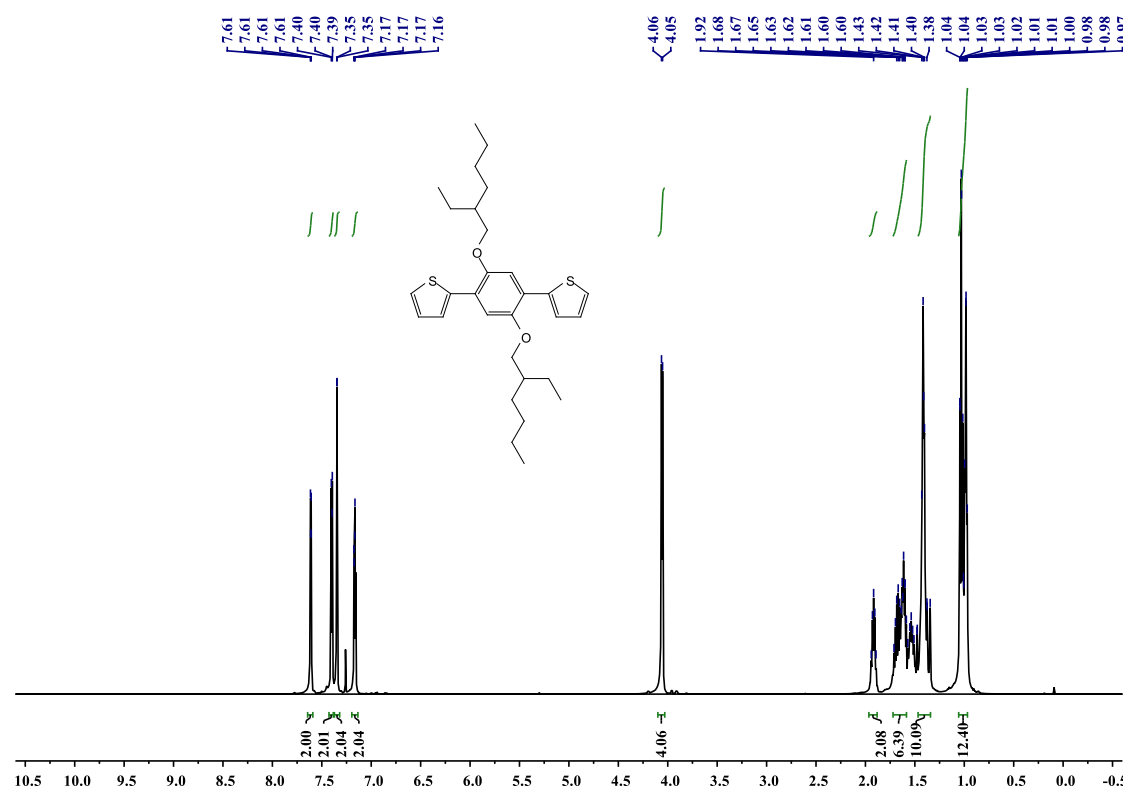


**Fig. S1** <sup>1</sup>H NMR spectrum of TBT at 293K in CDCl<sub>3</sub>.

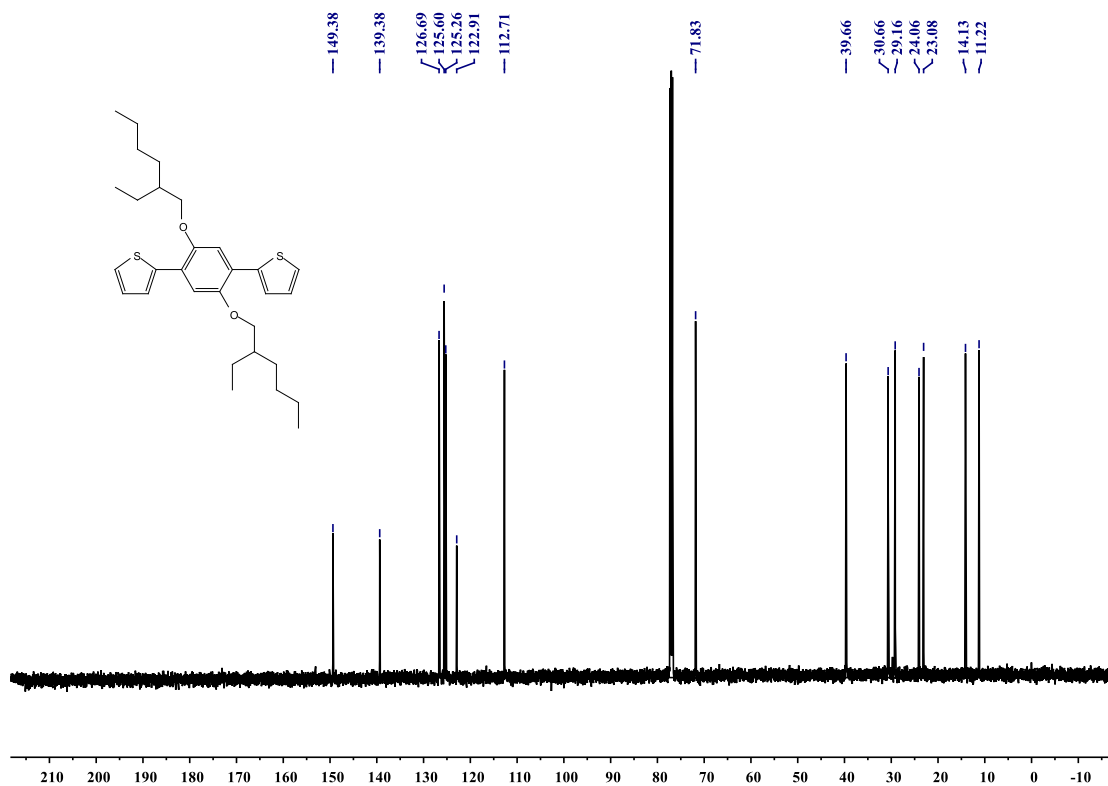
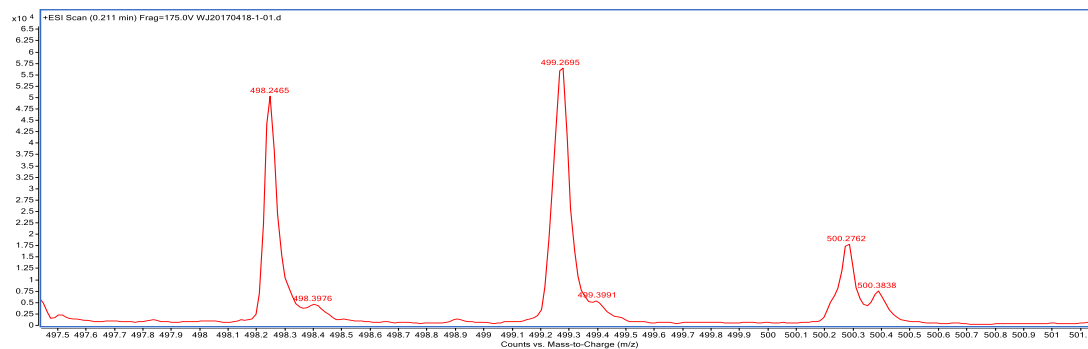
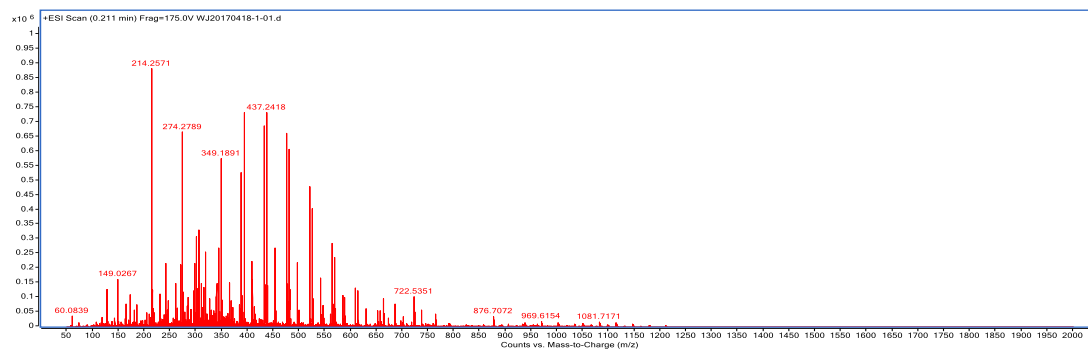


**Fig. S2** <sup>13</sup>C NMR spectrum of TBT at 293K in CDCl<sub>3</sub>.



Formula (M)	Score (MFG)	Mass	Mass (MFG)	m/z (Calc)	Diff (ppm)	DBE	m/z
C <sub>30</sub> H <sub>42</sub> O <sub>2</sub> S <sub>2</sub>	100	498.2622	498.2626	499.2699	0.8	10	499.2695

Fig. S3 HRMS spectra of TBT.

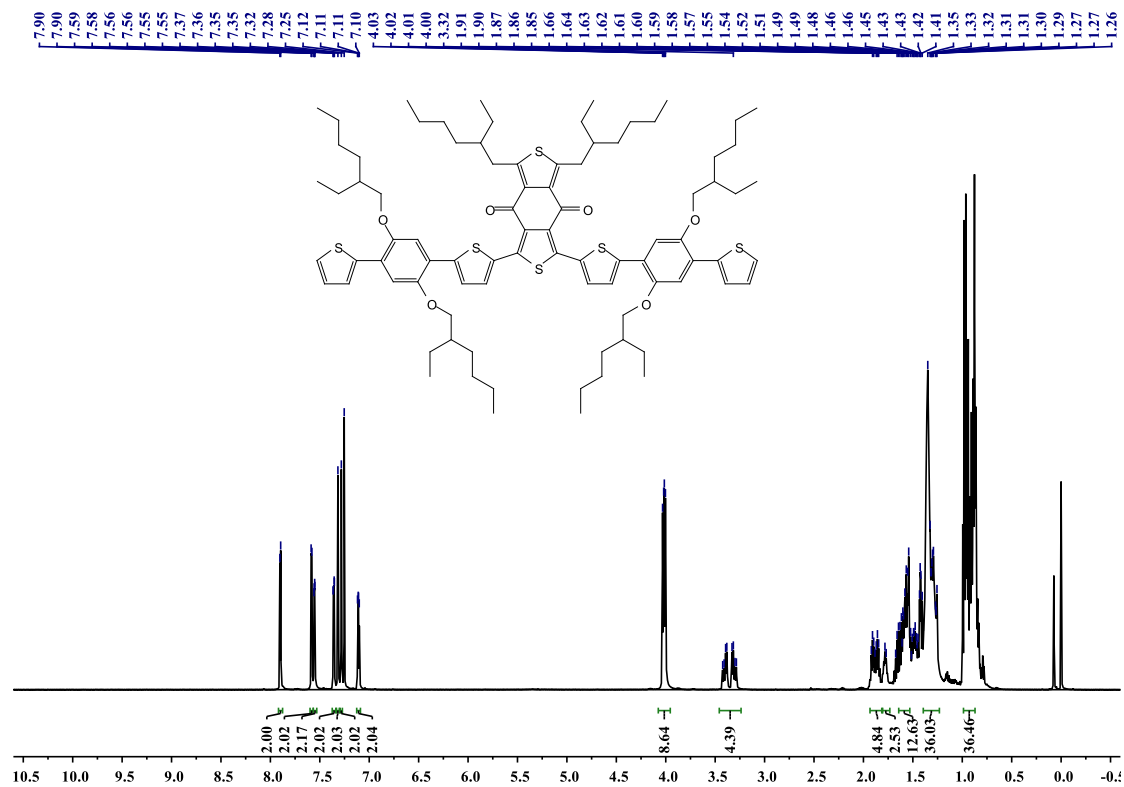


Fig. S4 <sup>1</sup>H NMR spectrum of DTBTBDD at 293K in CDCl<sub>3</sub>.

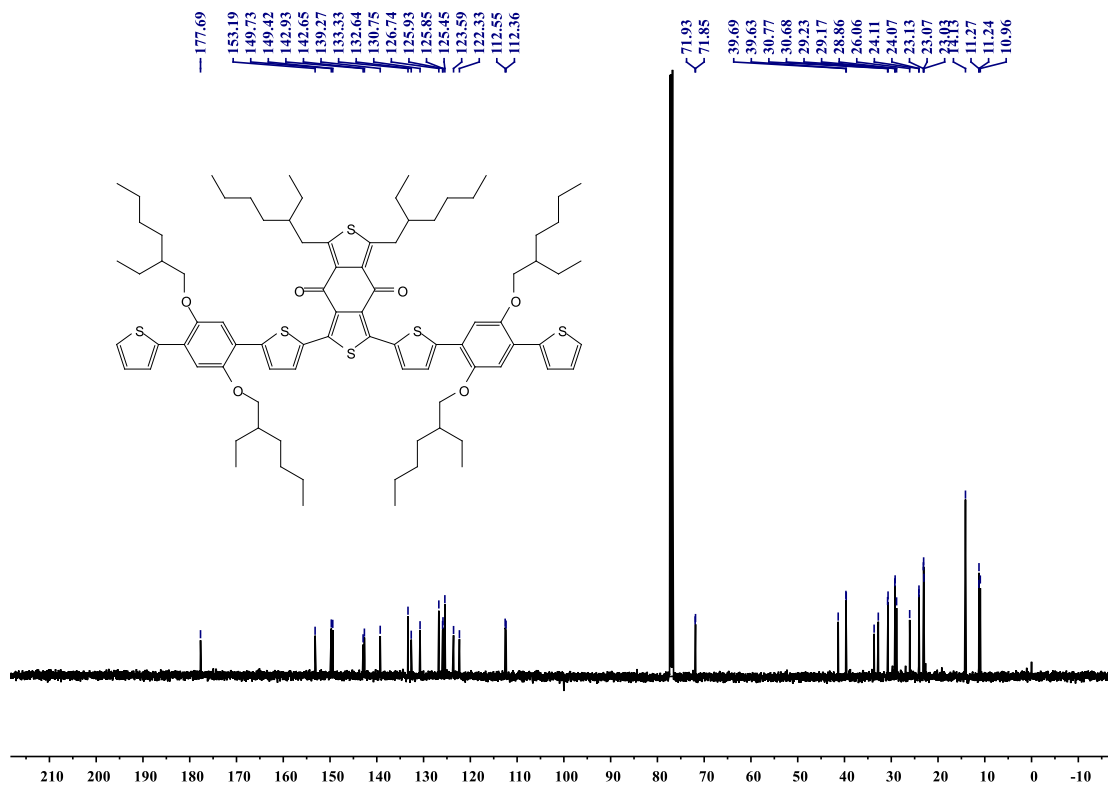
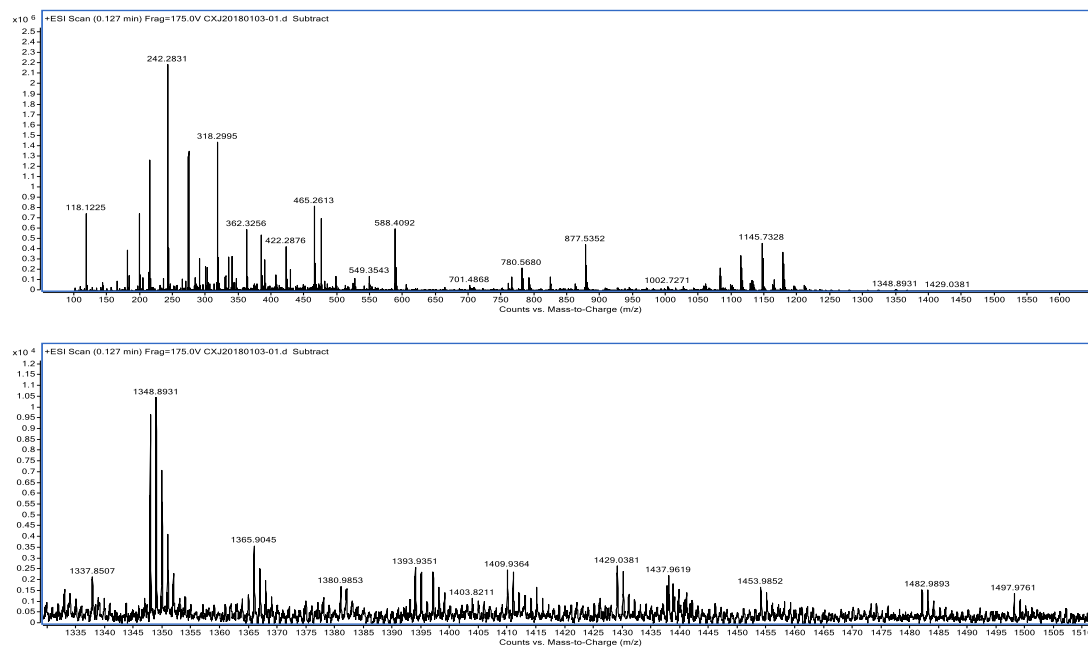


Fig. S5  $^{13}\text{C}$  NMR spectrum of DTBTBDD at 293K in  $\text{CDCl}_3$ .



Formula (M)	Score (MFG)	Mass	Mass (MFG)	m/z (Calc)	Diff (ppm)	DBE	m/z
$\text{C}_{86}\text{H}_{116}\text{O}_6\text{S}_6$	99.98	1438.23	1438.3383	1438.3697	2.8	30	1438.7130

Fig. S6 HRMS spectra of DTBTBDD.

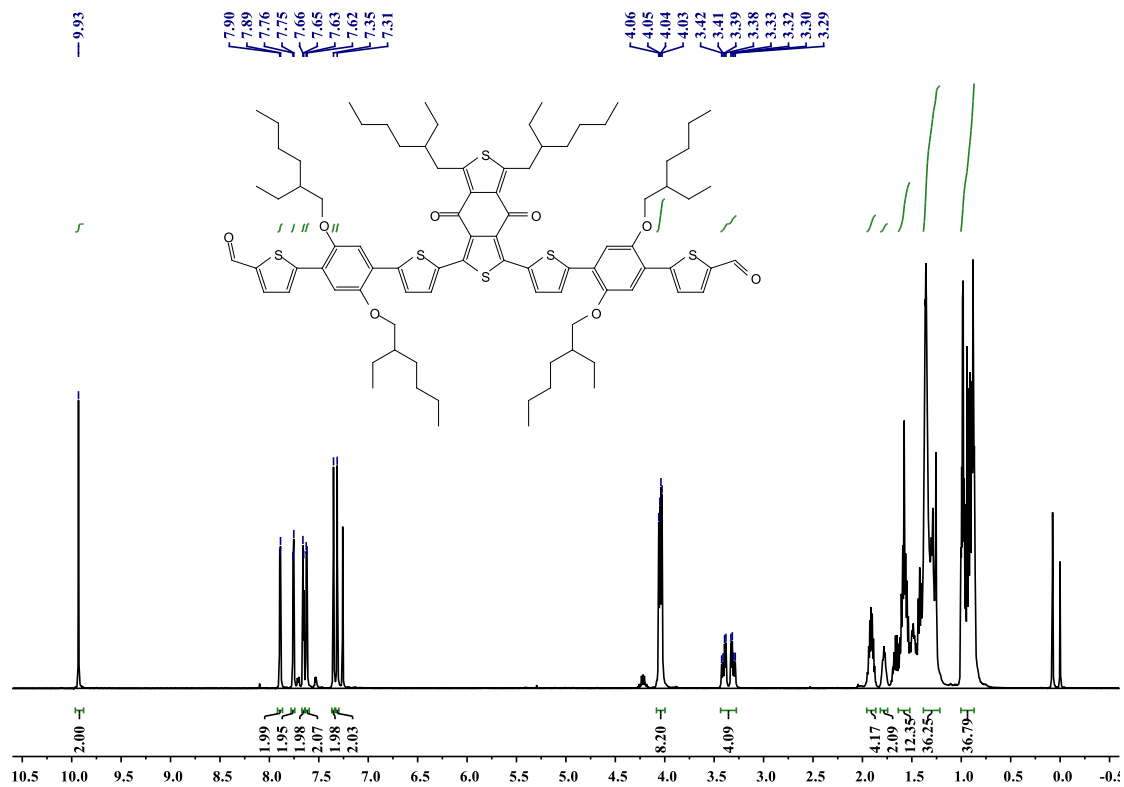


Fig. S7  $^1\text{H}$  NMR spectrum of DCHOTBTBDD at 293K in  $\text{CDCl}_3$ .

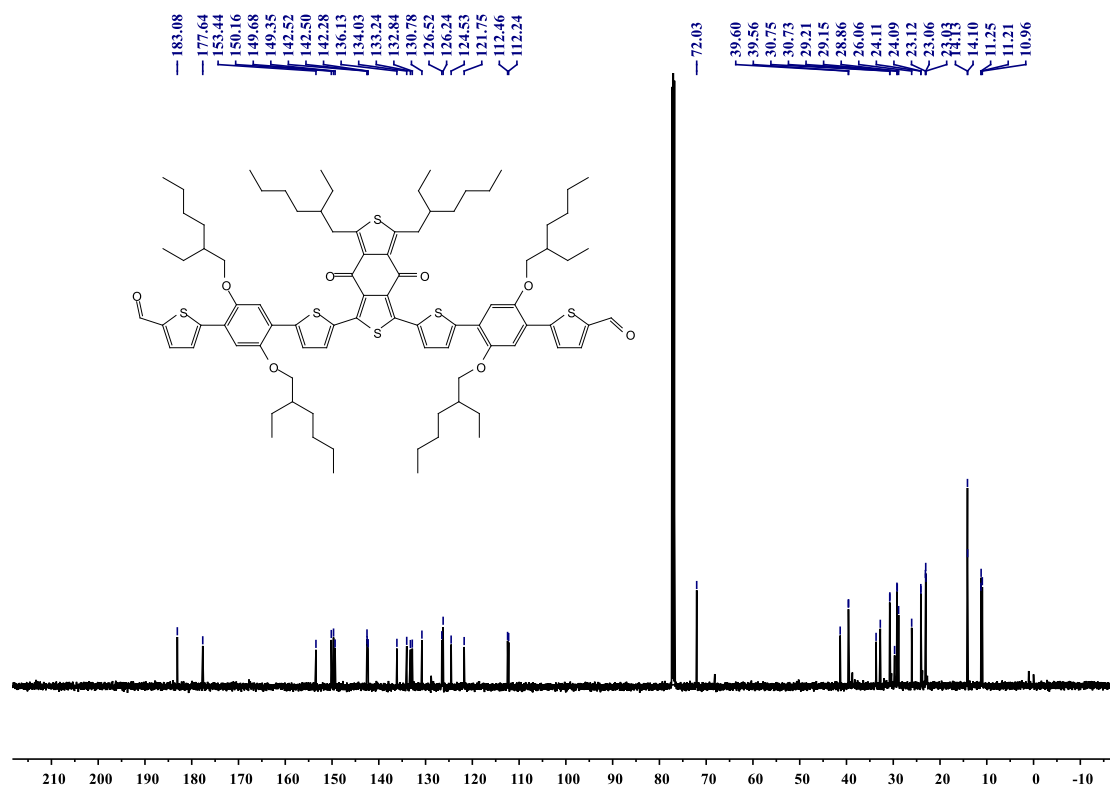
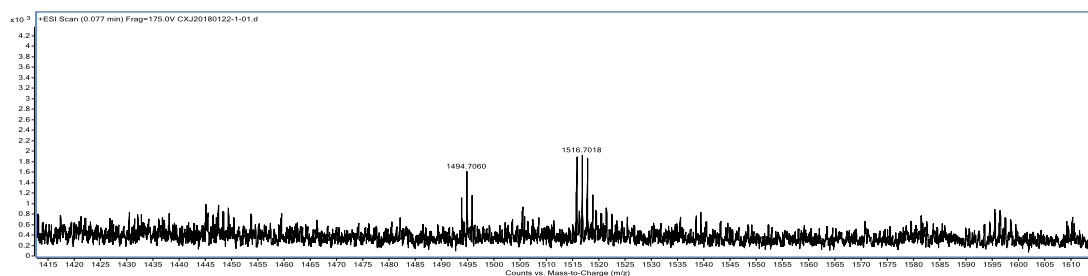
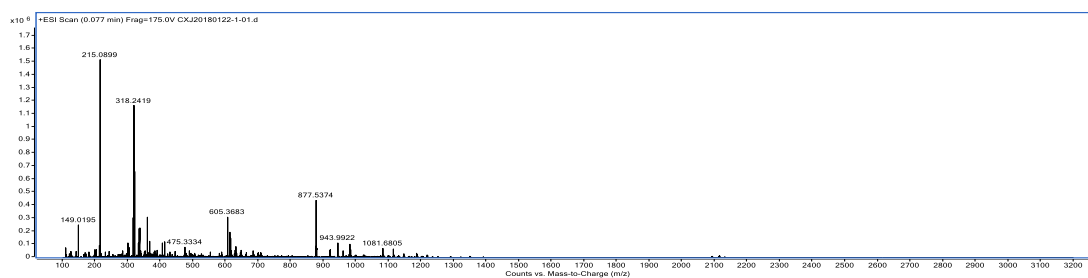


Fig. S8  $^{13}\text{C}$  NMR spectrum of DCHOTBTBDD at 293K in  $\text{CDCl}_3$ .



Formula (M)	Score (MFG)	Mass	Mass (MFG)	m/z (Calc)	Diff (ppm)	DBE	m/z
C <sub>88</sub> H <sub>116</sub> O <sub>8</sub> S <sub>6</sub>	99.95	1494.23	1494.3383	1494.2526	1.6	65	1494.7028

Fig. S9 HRMS spectra of DCHOTBTBDD.

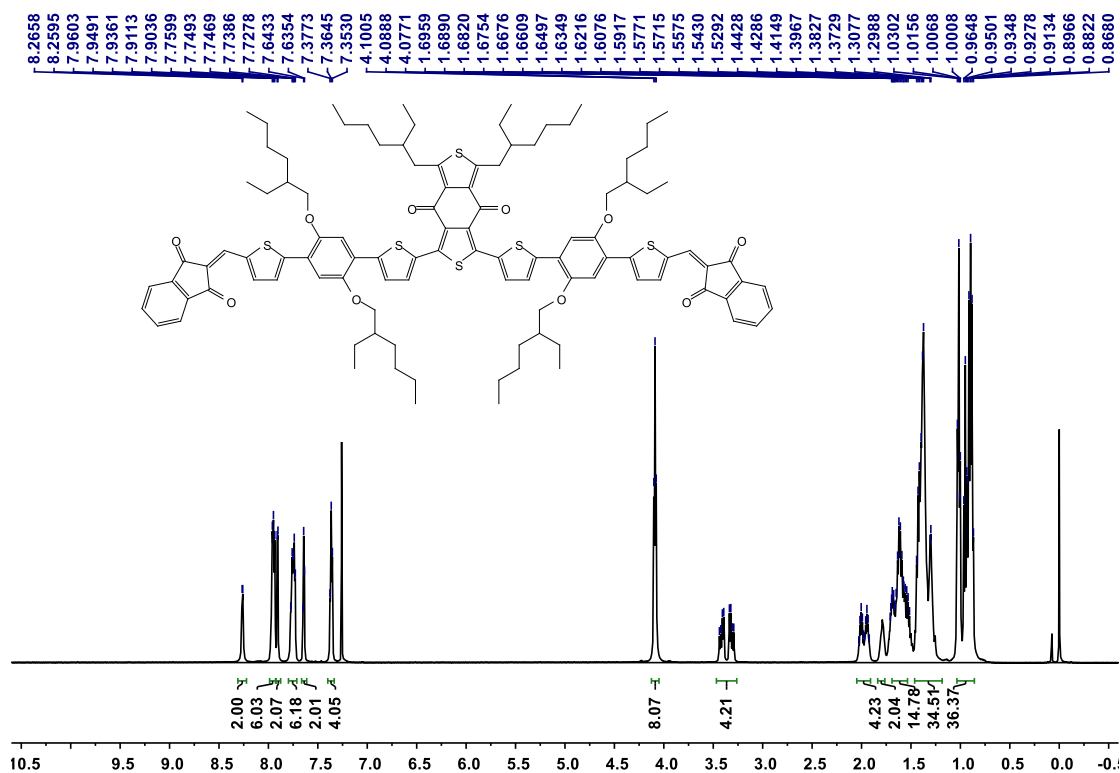
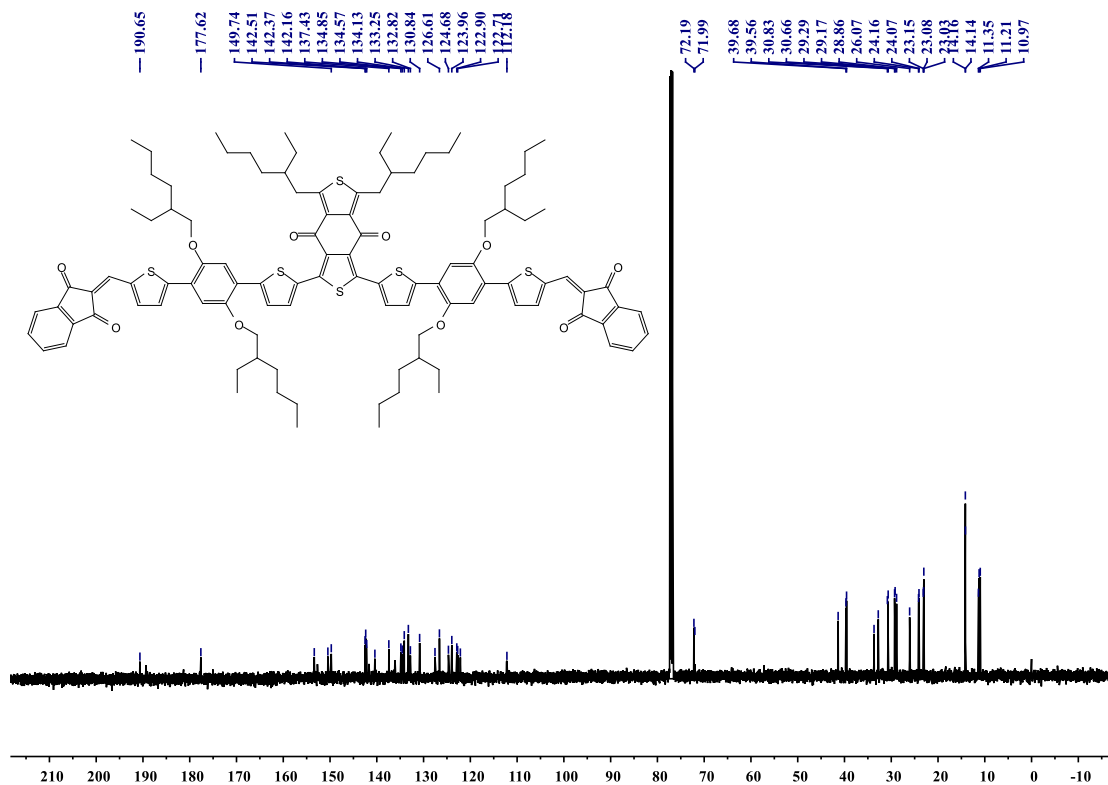
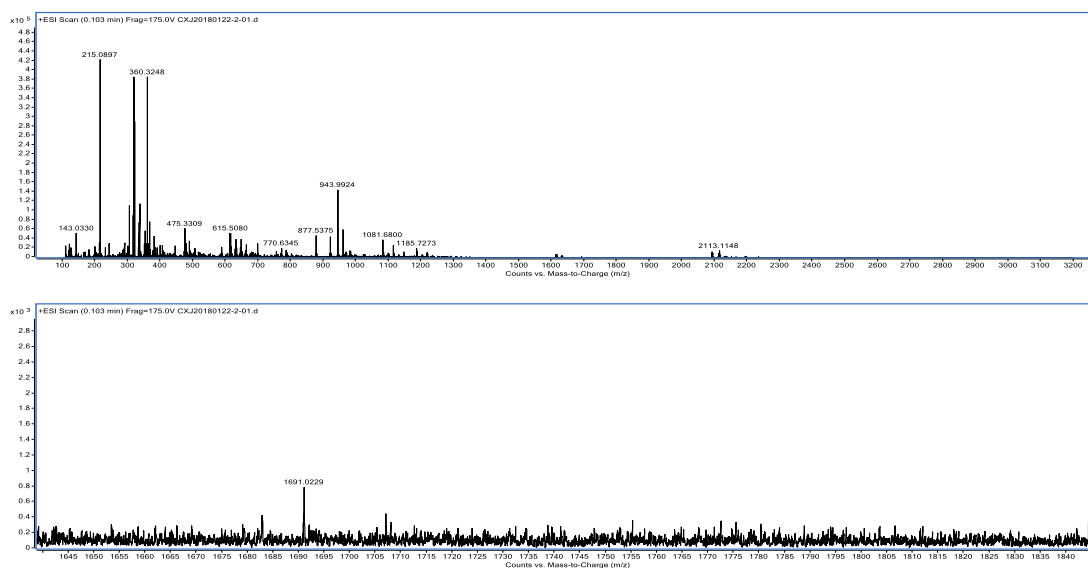


Fig. S10 <sup>1</sup>H NMR spectrum of BDD-IN at 293K in CDCl<sub>3</sub>.



**Fig. S11**  $^{13}\text{C}$  NMR spectrum of BDD-IN at 293K in  $\text{CDCl}_3$ .



Formula (M)	Score (MFG)	Mass	Mass (MFG)	m/z (Calc)	Diff (ppm)	DBE	m/z
$\text{C}_{106}\text{H}_{124}\text{O}_{10}\text{S}_8$	99.99	1750.2373	1750.7140	1750.5176	8.9	14	1750.7548

**Fig. S12** HRMS spectra of BDD-IN.

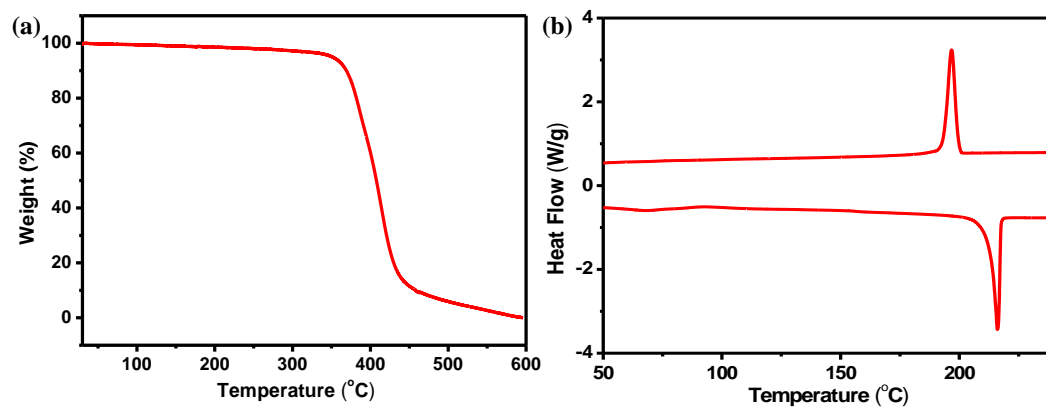


**Fig. S13** (a) TGA curve of BDD-IN. (b) DSC thermograms of BDD-IN with a heating rate of  $10\text{ }^{\circ}\text{C min}^{-1}$  under  $\text{N}_2$ . The lower lines and the upper lines are from the heating scans and cooling scans, respectively.

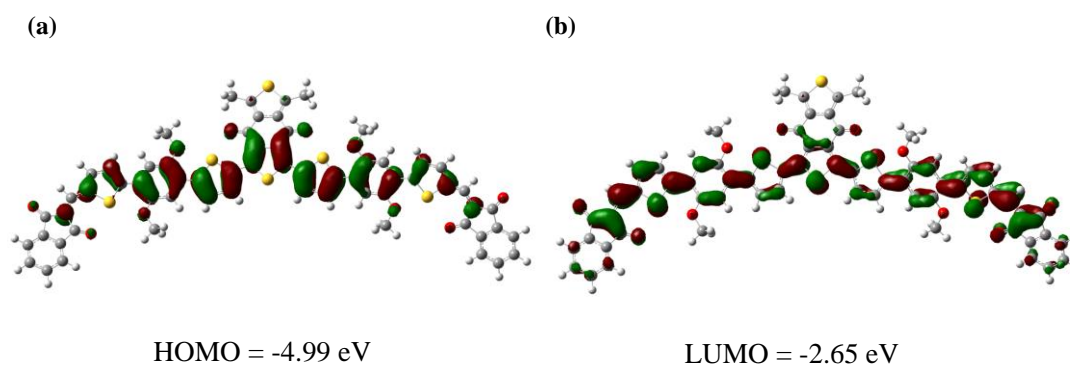


**Fig. S14** Frontier molecular orbitals of BDD-IN using DFT evaluated at the B3LYP/6-31G(d) level of theory.

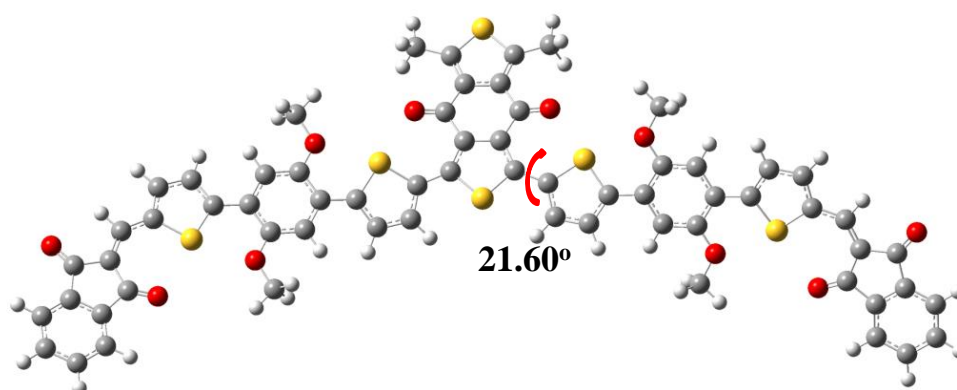


**Fig. S15** Optimized molecular geometries of BDD-IN using DFT evaluated at the B3LYP/6-31G(d) level of theory.

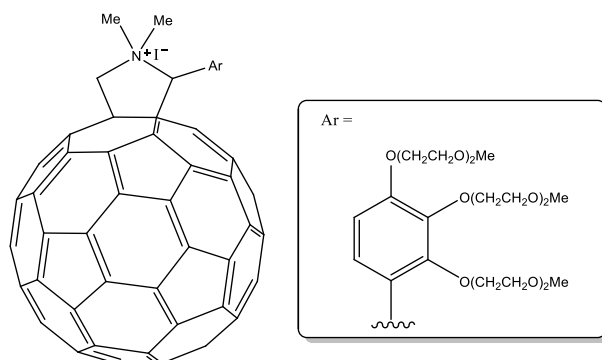


**Fig. S16** Chemical structure of PrC<sub>60</sub>MA.

Photovoltaic parameters of BDD-IN:PC<sub>71</sub>BM based devices.

**Table S1** Photovoltaic parameters of BDD-IN:PC<sub>71</sub>BM based devices with donor concentration of 8 mg/mL and donor/acceptor weight ratio of 1:0.8.

Treatment	$V_{oc}/V$	$J_{sc}/\text{mA cm}^{-2}$	FF/%	PCE/%
None	1.10	6.01	30.3	2.00
TA (120 °C)	0.98	6.69	35.2	2.32
SVA (60 s)	0.96	10.66	76.3	7.70

**Table S2** Photovoltaic parameters of BDD-IN:PC<sub>71</sub>BM based devices with donor concentration of 10mg/ml and donor/acceptor weight ratio of 1:0.8 with different SVA time.

Treatment	$V_{oc}/V$	$J_{sc}/\text{mA cm}^{-2}$	FF/%	PCE/%
None	1.042	5.75	28.3	1.70
SVA (60 s)	0.974	12.00	69.2	8.09
SVA (90 s)	0.965	12.44	72.3	8.70
SVA (110 s)	0.964	12.04	71.3	8.39

**Table S3** Photovoltaic parameters of BDD-IN:PC<sub>71</sub>BM based devices with donor concentration of 10mg/ml and donor/acceptor weight ratio of 1:0.8 with different spin-speed.

Spin-speed	$V_{oc}/V$	$J_{sc}/\text{mA cm}^{-2}$	FF/%	PCE/%
1300rpm	0.953	11.97	71.2	8.11
1700rpm	0.965	12.44	72.3	8.70
2100rpm	0.952	12.30	71.9	8.42

**Table S4** Photovoltaic parameters of BDD-IN:PC<sub>71</sub>BM based devices with different concentration of DIO.

Concentration (v:v, %)	$V_{oc}/V$	$J_{sc}/\text{mA cm}^{-2}$	FF/%	PCE/%
0.3	0.964	10.41	68.2	6.85
0.5	0.960	11.07	71.0	7.55
0.7	0.895	6.86	41.1	2.52
1	0.740	1.32	22.4	0.22

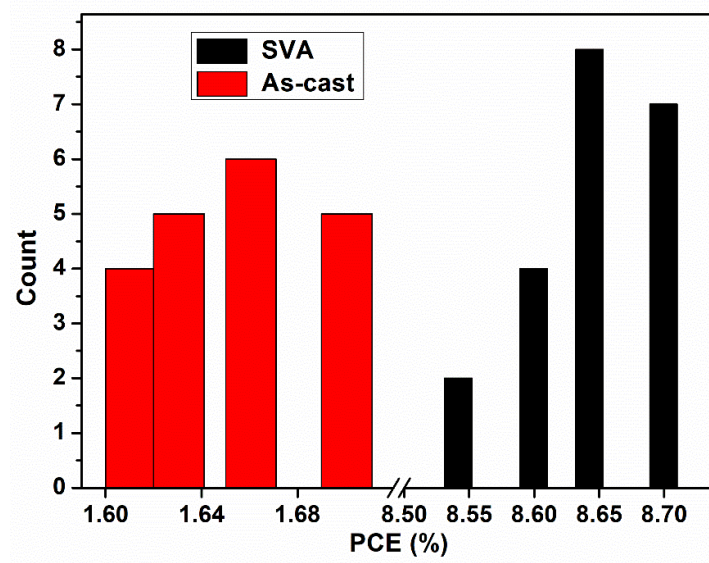


**Fig. S17** The statistical histogram of PCEs for BDD-IN:PC<sub>71</sub>BM based devices (20 devices for each case under the as-cast or SVA-treated conditions).

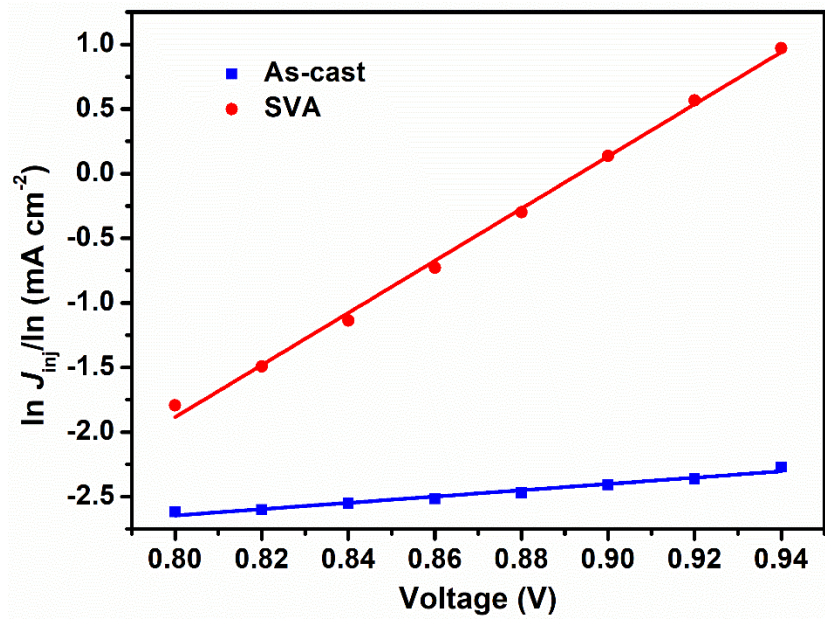


**Fig. S18** The fitted dark injected current ( $J_{inj}$ ) versus voltage ( $V$ ) for BDD-IN:PC<sub>71</sub>BM devices with different treatment<sup>a)</sup>.

<sup>a)</sup>The dark injected current ( $J_{inj}$ ) versus voltage ( $V$ ) for BDD-IN:PC<sub>71</sub>BM devices was exponentially fitted according to Equation 2, therefore to determine the reverse saturation current density  $J_{0,n}$ .<sup>3, 4, 5.</sup>

$$J_{inj} = J_{0,n} \exp\left(\frac{qV}{nkT}\right) \quad (2)$$

**Table S5** Measured and simulated performance parameters for BDD-IN:PC<sub>71</sub>BM blend films with different treatments<sup>b)</sup>.

Treatment	$V_{oc}$ (V)	$J_{0,n}$ (mA cm <sup>-2</sup> )	$J_{so}$ (mA cm <sup>-2</sup> )
As-cast	1.042	0.01	0.07
SVA	0.965	$1.48 \times 10^{-8}$	0.15

<sup>b)</sup>  $J_{so}$  was calculated according to Equation 3.

$$J_{0,n} = J_{so} \exp\left(\frac{-\Delta E_{DA}}{2nkT}\right) \quad (3)$$

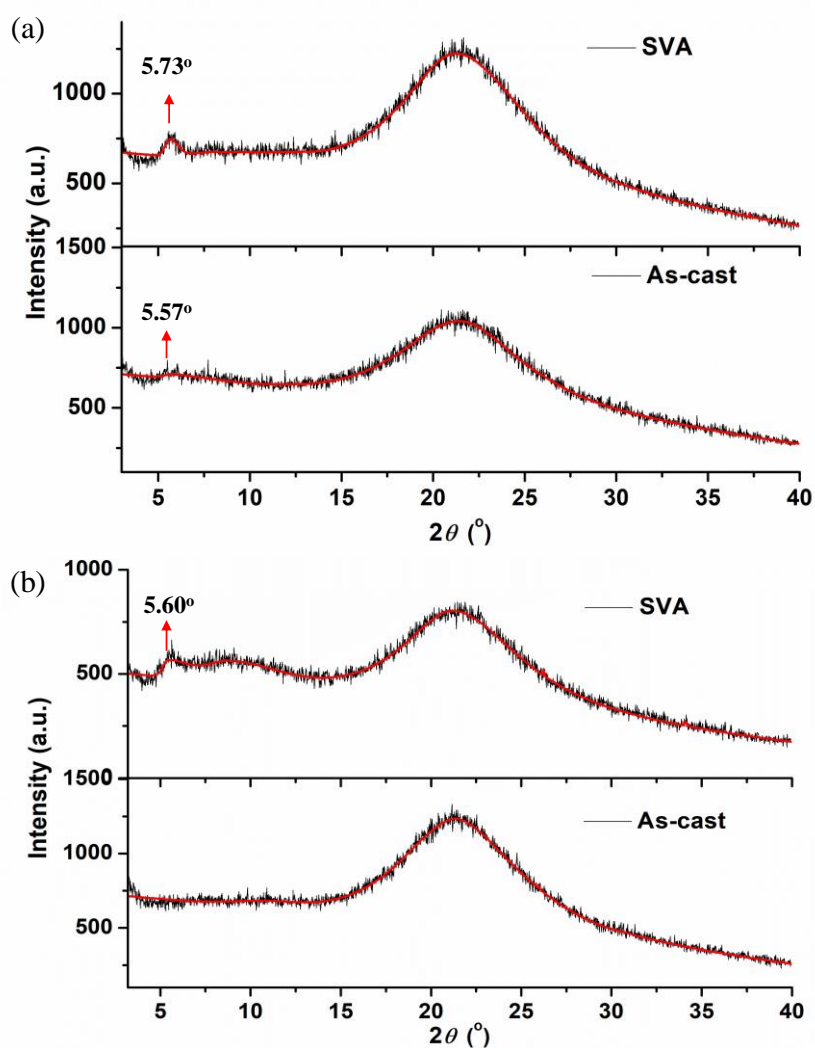


**Fig. S19** XRD patterns of pristine BDD-IN films (a) and BDD-IN:PC<sub>71</sub>BM films spin-coated from chloroform onto silicon substrates. Red lines are the fitting lines.

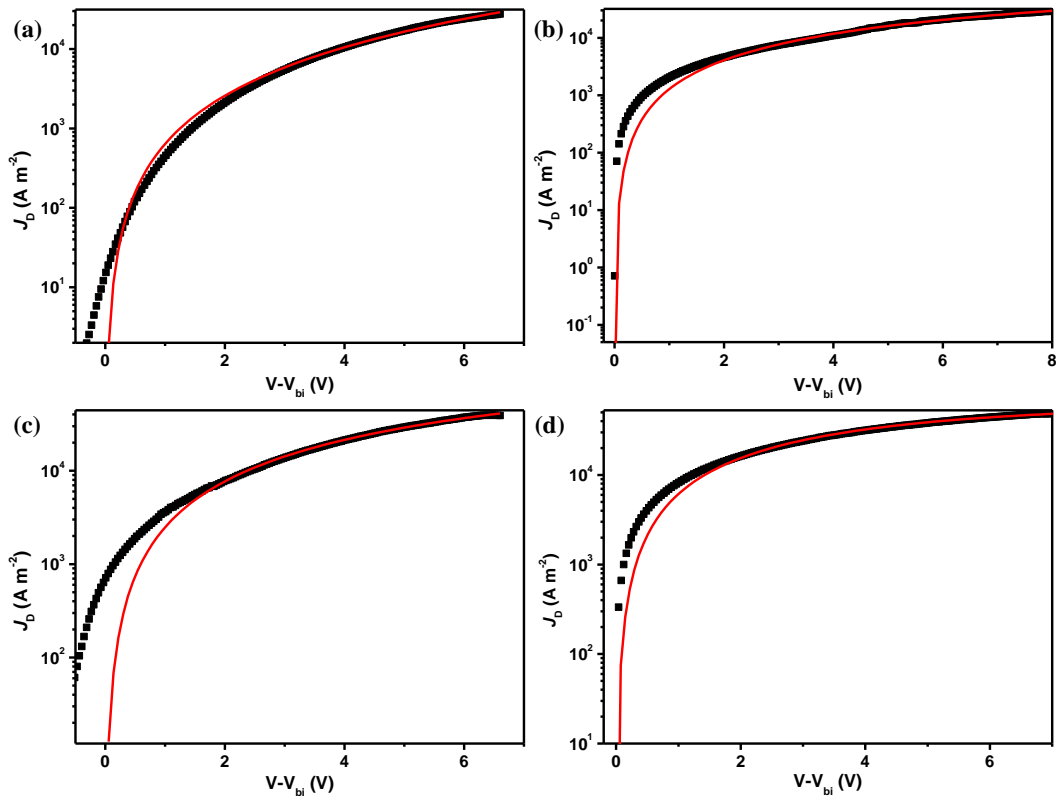


**Fig. S20** Experimental dark-current densities for as-cast BDD-IN:PC<sub>71</sub>BM based devices (a) hole mobility (b) electron mobility; SVA-treated BDD-IN:PC<sub>71</sub>BM based devices (c) hole mobility (d) electron mobility. The solid lines represent the fit using a model of single carrier SCLC with field-independent mobility. The  $J_D$ - $V$  characteristics are corrected for the built-in voltage  $V_{bi}$  that arises from the work function difference between the contacts.

## References

- (1) P. N. Murgatroyd, *J. Phys. D: Appl. Phys.*, 1970, **3**, 151-156.
- (2) S. M. Tuladhar, D. Poplavskyy, S. A. Choulis, J. R. Durrant, D. D. C. Bradley, J. Nelson, *Adv. Funct. Mater.*, 2005, **15**, 1171-1182.
- (3) K. Vandewal, K. Tvingstedt, A. Gadisa, O. Inganäs, J. V. Manca, *Nat. Mater.*, 2009, **8**, 904-909.
- (4) C. W. Schlenker, M. E. Thompson, *Chem. Commun.*, 2011, **47**, 3702-3716.
- (5) M. Li, F. Liu, X. Wan, W. Ni, B. Kan, H. Feng, Q. Zhang, X. Yang, Y. Wang, Y. Zhang, Y. Shen, T. P. Russell, Y. Chen, *Adv. Mater.*, 2015, **27**, 6296-6302.